JOURNAL OF CATALYSIS 50, 419–428 (1977)

# Dehydrogenation and Hydrogenation Activity of Palladium–Tin–Silica and Nickel–Tin–Silica

MITSUO MASAI,* KUNIHIKO HONDA,*[,1] AKINORI KUBOTA,*[,2] SHINJI OHNAKA,*[,3]
YUTAKA NISHIKAWA,*[,4] KEISUKE NAKAHARA,* KOSAKU KISHI,†
AND SHIGERO IKEDA†

*Department of Chemical Engineering, Faculty of Engineering, Kobe University, Rokkodai-cho, Nada-ku, Kobe, 657, and †Department of Chemistry, Osaka University, Toyonaka-shi, Osaka, 560, Japan

Received July 26, 1976; revised July 25, 1977

The dehydrogenation of cyclohexanone, cyclohexylamine, cyclohexane, and 2-propanol and the hydrogenation of ethylene on palladium–tin–silica and the hydrogenation of benzene on nickel–tin–silica were studied. With nickel–silica and nickel–tin–silica, the deposition of carbonaceous materials was studied kinetically. The X-ray photoelectron spectra of palladium–tin and nickel–tin were observed. The catalytic activities of both of the catalyst systems changed in similar ways with the change of the Pd/Sn and Ni/Sn ratios (atomic) of the catalysts. The dehydrogenation activity increased to a maximum and then decreased, with a decrease in the Pd/Sn and Ni/Sn ratios. The hydrogenation activity of the tin-containing catalysts was much lower than that of the tin-free catalysts. Carbonaceous materials were observed to be deposited more easily on the nickel–silica than on the nickel–tin–silica. The palladium-4d and nickel-3d band peaks of the alloy systems obtained by X-ray photoelectron spectroscopy were observed to shift to higher binding energies as the Pd/Sn and Ni/Sn ratios decreased. From the amount of carbon monoxide adsorbed, the surface concentration of palladium and that of nickel on the catalysts were suggested to be the minor determining factor of the catalytic activity studied here. It is concluded that tin is not just a diluent for the active metal but is an effective component to weaken the adsorption bond.

## INTRODUCTION

The nickel–tin–silica catalysts have been reported to show high activity in the dehydrogenation of cyclohexanol and cyclohexanone to phenol by Swift and Bozik (*1*). On these catalysts, the dehydrogenation reactions, such as cyclohexanone to phenol, cyclohexylamine to aniline, cyclohexane to benzene, and 2-propanol to acetone, were studied by two of the present authors (M. M. and S. O.), and the optimum nickel-to-tin atomic ratio (Ni/Sn) was observed, i.e., Ni/Sn = 2.5 for cyclohexanone (*1*, *2*), 8 for cyclohexylamine and 2-propanol, and 10 for cyclohexane (*2*). The presence of narrow-range alloy phases was observed in addition to the metallic nickel and β-tin, i.e., NiSn (*1*, *2*), $Ni_3Sn_4$, and $Ni_3Sn_2$ (*2*). These alloy phases have been considered to

---

[1] Present address: Fuji Photo Film Co., Ltd., Nakanuma 210, Minami-Ashigara-shi, Kanagawa-ken, 250-01, Japan.

[2] Present address: Sumitomo Rubber Industries, Ltd., Tsutsui-cho 1-1-1, Fukiai-ku, Kobe, 651, Japan.

[3] Present address: Kawaken Fine Chemicals Co., Ltd., Imafuku-Nakadai 2835, Kawagoe-shi, Saitama-ken, 356, Japan.

[4] Present address: Mitsubishi Plastics Industries, Ltd., Mitsuya-cho 5-8, Nagahama-shi, Shiga-ken, 526, Japan.

ISSN 0021-9517

TABLE 1

Surface Area of Calcined Palladium–Tin–Silica

| Pd/Sn | Surface area ($m^2/g$) |
|---|---|
| ∞ | 240 |
| 3 | 230 |
| 1 | 250 |
| 0.3 | 243 |

make the adsorption bond weak, and this weakening probably improves the dehydrogenation activity (*2*).

This improvement of the catalytic activity of nickel alloyed with tin is studied extensively in the present work. The catalytic activity of the palladium–tin–silica was compared with that of the nickel–tin–silica. The palladium–tin alloy system, like the nickel–tin system, shows a complex phase diagram, and the presence of $Pd_3Sn$, $Pd_2Sn$, $Pd_3Sn_2$, PdSn, $PdSn_2$, $PdSn_3$, and $PdSn_4$ is accepted (*3*). Therefore, it is expected that the mixed alloy phases are present on catalyst carriers like the nickel–tin–silica. The valence band spectra of palladium–tin and nickel–tin were observed by X-ray photoelectron spectroscopy (XPS) using alloy plates. The valence band spectra of nickel–germanium, iron–germanium, and gold–germanium were measured by XPS by two of the present authors (K. K. and S. I.) (*4*). These transition metal–germanium systems showed a shift of nickel, iron, and gold valence band peaks to higher binding energies (*4*).

## METHODS

The palladium–tin–silica and the palladium–silica catalysts were prepared by soaking silica hydrogel in a solution of metal salts. The details of the preparation have been described elsewhere (*2*). Palladium nitrate was dissolved in concentrated nitric acid. The total metal component (Pd + Sn) was ca. 11 wt% of the total weight of the catalyst. The Pd/Sn atomic ratios were 0.3, 1, 3, and ∞ (palladium–silica).

The surface area of the calcined catalysts was measured by BET method using nitrogen as an adsorbate at the boiling point of liquid nitrogen. The results are shown in Table 1.

The catalysts were reduced at 923 K in flowing hydrogen for 3 hr just before the reaction experiments. The amount of adsorbed carbon monoxide was measured immediately after the reduction by the flow method using helium as a carrier gas at 195 K.

The X-ray diffraction patterns of the reduced catalysts were obtained by a Rigaku–Denki Geigerflex wide-angle diffractometer using Ni-filtered Cu$K\alpha$ radiation.

The reaction experiments were performed in the same way as before (*2*). Detailed conditions are described in each figure and table.

The deposition of carbonaceous materials on the catalyst was studied kinetically by using Shimadzu MDB-10 high-sensitivity electronic thermal microbalance. 1-Butene was used as a source of carbonaceous materials and the catalysts studied were of Ni/Sn = ∞ and of Ni/Sn = 8. Deposition of carbonaceous materials was performed at the normal pressure and 673–873 K. The catalyst was hung in the thermal microbalance through which 1-butene was fed, and the feed rate was 48 g of catalyst/h/mol of $C_4H_8$ in the section of hung catalyst. The feed was composed of 7.6 parts of hydrogen and 1 part 1-butene. The slope of the weight-increase curve in the initial 30 min was defined as the rate of deposition.

XPS spectra were obtained by an AEI-ES200 electron spectrometer at ca. $1.3 \times 10^{-5}$ Pa with a scanning interval of 0.1 eV. The sample was excited by Al$K\alpha_{1,2}$ radiation. The output of the spectrometer was the sum of multiple scannings. The details of the operation have been described elsewhere (*4*).

Samples for XPS were alloy plates of

palladium–tin and nickel–tin. The alloy plates were obtained by melting the known mixtures of palladium and tin and of nickel and tin at 1873 K in quartz ampoules sealed *in vacuo*. The melted metals were cooled very slowly (ca. 48 hr). The alloy blocks were cut into suitable sizes for the electron spectrometer by using a diamond cutter. They were reduced at 623 K in hydrogen for 3 hr and were sealed respectively in a Pyrex ampoule after evacuation to 1.3 × $10^{-4}$ Pa. The ampoule was broken just before the XPS measurement, and the sample plate was set on the sample holder. The sample was again reduced in a hydrogen stream (3 × $10^{4}$ Pa) at 423 K for 1 hr in a preparation chamber, cooled, and transferred into the ionization chamber (ca. $10^{-5}$ Pa) after evacuation. On the energy scale, the Fermi level was estimated using palladium film in the usual way.

Reagents and metals, of *Guaranteed Reagents* grade or comparable to that quality, were obtained from Wako Pure Chemical Industries, Ltd. (Osaka). The purity of metallic palladium, nickel, and tin was ca. 99.8, 99.7, and 99.99%, respectively. Gases were obtained commercially.

## RESULTS

### *Dehydrogenations on Palladium–Tin–Silica*

Phenol was the major product of the dehydrogenation of cyclohexanone. Benzene was detected as the only minor product. Figure 1 shows the decrease of the conversion (mole percentage) of cyclohexanone in connection with the reaction time. Selectivity (mole percentage) of phenol is shown in Table 2.

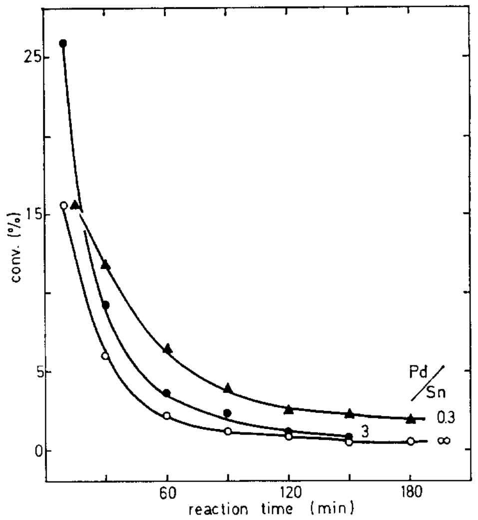

FIG. 1. Decrease in the conversion vs reaction time in dehydrogenation of cyclohexanone on Pd–Sn–silica catalysts at 753 K; W/F = 116 g of catalyst·hr/g-mol of reactant; $H_2/C_6H_{10}O$ = 10 (molar ratio).

Aniline was the major product of the dehydrogenation of cyclohexylamine. Benzene was the minor product. Figure 2 shows the decrease of the conversion of cyclohexylamine in connection with the reaction time. Selectivity of aniline is shown in Table 2.

TABLE 2

Selectivity of Dehydrogenation of Cyclohexanone and Cyclohexylamine

| Pd/Sn | Reaction time (min) | Cyclo-$C_6H_{10}O \rightarrow C_6H_5OH$ (mol% of phenol) | Reaction time (min) | Cyclo-$C_6H_{11}NH_2 \rightarrow C_6H_5NH_2$ (mol% of aniline) |
|---|---|---|---|---|
| ∞ | 10 | 97.3 | 10 | 98.3 |
| | 90 | ~100 | 30 | 97.4 |
| 3 | 10 | 98.0 | 30 | 99.1 |
| | 90 | 94.2 | 120 | ~100 |
| 0.3 | 30 | 96.4 | 30 | 38.5 |
| | 90 | 80.0 | | |

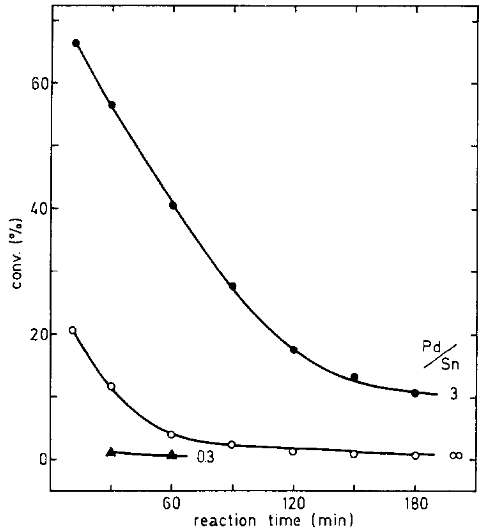

FIG. 2. Dehydrogenation of cyclohexylamine on Pd–Sn–silica at 673 K; W/F = 136 g of catalyst·hr/g-mol of reactant; $H_2/C_6H_{11}NH_2$ = 10.

Benzene was the only product of the dehydrogenation of cyclohexane. Figure 3 shows the decrease of the conversion of cyclohexane in connection with the reaction time.

Acetone was the only product of the dehydrogenation of 2-propanol. Figure 4 shows the decrease of the conversion of 2-propanol in connection with the reaction time.

The four dehydrogenation reactions described above have been studied previously on nickel–tin–silica (*2*). The variation in catalytic activity in connection with the composition of the catalyst in the present work is similar to that in the previous work (*2*). The tin in palladium–tin–silica shows a promoting effect on the dehydrogenation activity as was shown in the case of the nickel–tin–silica. The observed optimum Pd/Sn is 3 for the dehydrogenation of cyclohexylamine and cyclohexane and 0.3 for the dehydrogenation of cyclohexanone and 2-propanol. The tin–silica catalyst showed no activity for the four reactions (*2*).

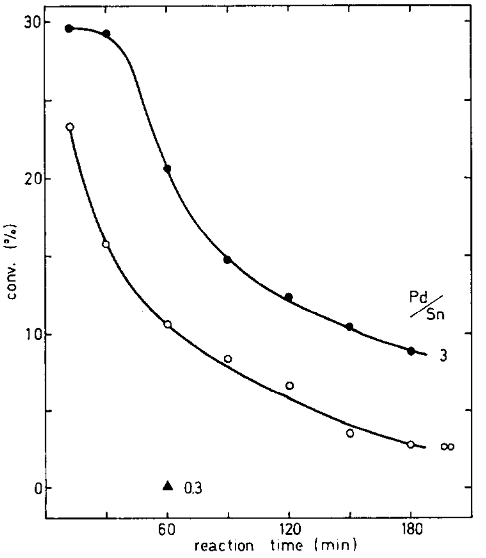

FIG. 3. Dehydrogenation of cyclohexane on Pd–Sn–silica at 723 K; W/F = 100 g of catalyst·hr/g-mol of reactant; $H_2/C_6H_{12}$ = 10.

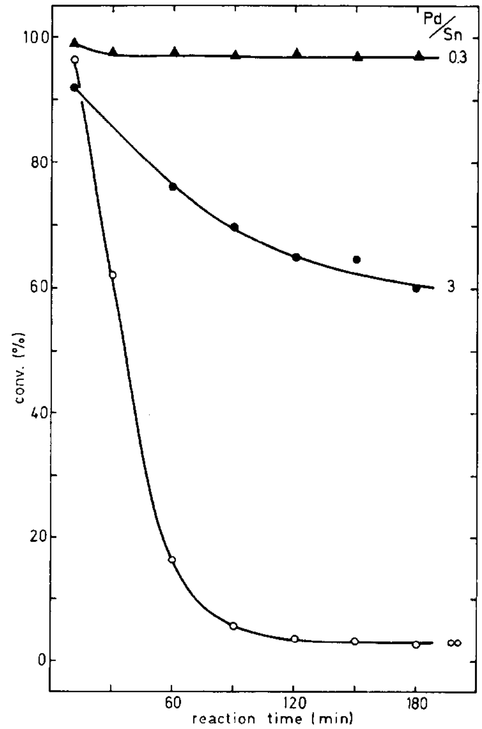

FIG. 4. Dehydrogenation of 2-propanol on Pd–Sn–silica at 723 K; W/F = 52 g of catalyst·hr/g-mol of reactant; $H_2/C_3H_7OH$ = 5.

### *Deposition of Carbonaceous Materials*

The hydrocracking reaction proceeded under the above-mentioned conditions. Activation energy was obtained from the slope of the logarithm of the deposition rate vs the reciprocal of temperature (kelvin). The results shown in Table 3 indicate that the deposition of carbonaceous materials on nickel–silica is easier than on nickel–tin–silica.

### *Hydrogenation of Ethylene and Benzene*

The hydrogenation of ethylene to ethane was performed on the palladium–tin–silica, and that of benzene to cyclohexane on the nickel–tin–silica. Ethane was the only product of the former reaction, and cyclohexane was the only product of the latter. As Table 4 shows, hydrogenation reactions proceeded nearly to completion on the palladium–silica and on the nickel–silica under conditions by which moderate results were obtained on the tin-containing catalysts.

### *Adsorption of Carbon Monoxide*

Table 5 shows the amount of carbon monoxide adsorbed on the palladium–tin–silica and on the nickel–tin–silica. A decrease in the surface concentrations of palladium and nickel may be inferred from Table 5. The tin–silica showed no adsorption under this condition.

TABLE 3

Activation Energy of the Deposition of Carbonaceous Materials

| Catalyst | Activation energy (kJ/mol) |
|---|---|
| Ni/Sn = ∞ | 79 |
| Ni/Sn = 8 | 126 |

TABLE 4

Conversion of Hydrogenation of Ethylene (Pd–Sn–Silica)[a] and Benzene (Ni–Sn–Silica)[b]

| Pd/Sn | $C_2H_4 \rightarrow C_2H_6$ | Ni/Sn | $C_6H_6 \rightarrow$ cyclo-$C_6H_{12}$ |
|---|---|---|---|
| ∞ | ~100 | ∞ | ~100 |
| 3 | 84 | 10 | 14 |
| 1 | 80 | 8 | 9 |
| 0.3 | 28 | 2.5 | Not detected |

[a] Reaction conditions: W/F = 100 g of catalyst·hr/g-mol; $H_2/C_2H_4$ = 10 (mol/mol); 463 K; 60 min after start of reaction.

[b] Reaction conditions: W/F = 55 g of catalyst·hr/g-mol; $H_2/C_6H_6$ = 10; 453 K; 60 min after start of reaction.

### *X-Ray Diffraction Patterns*

Figure 5 shows the X-ray diffraction patterns of the palladium–tin–silica. Metallic palladium (*5*) was observed on palladium–silica. Metallic palladium, $Pd_3Sn_2$ (*6*), PdSn (*7*), and $PdSn_3$ (*8*) were observed on catalyst of Pd/Sn = 3. $Pd_3Sn_2$, PdSn, $PdSn_2$ (*9*), $PdSn_3$, and β-tin (*10*) were observed on the catalyst of Pd/Sn = 1. PdSn and β-tin were observed on the catalyst of Pd/Sn = 0.3. Only the PdSn phase was observed in all the palladium–tin–silica.

### *XPS Spectra*

Figures 6 and 7 show the valence band spectra of palladium–tin and nickel–tin, respectively. Figure 6 shows that the position of the main peak associated with the palladium-4d state shifts to higher binding energies as the Pd/Sn ratio decreases. Figure 7 shows a similar tendency for the position of the main peak associated with the nickel-3d state to that for the position of palladium-4d state, but the shift is less than that for palladium–tin.

## DISCUSSION

It has been reported that tin promotes the dehydrogenation activity of the nickel–silica catalyst if the Ni/Sn ratio is high (*2*). The similar effect for tin is observed with the palladium–tin–silica. A small amount of tin in the palladium–tin–silica promotes the dehydrogenation activity, and a large

TABLE 5

Amount of CO Adsorbed on Palladium–Tin–Silica and Nickel–Tin–Silica at 195 K

| Pd/Sn | Pd in metal part (atom %) | CO adsorbed ($\times 10^{19}$ molecules/g of catalyst) | Ni/Sn | Ni in metal part (atom %) | CO adsorbed ($\times 10^{19}$ molecules/g of catalyst) |
|---|---|---|---|---|---|
| ∞ | 100 | 5.1 | ∞ | 100 | 3.4 |
| 3 | 75 | 4.8 | 8 | 89 | 1.7 |
| 1 | 50 | 2.2 | 2.5 | 71 | 1.4 |
| 0.3 | 23 | 2.0 | 1 | 50 | 1.2 |
| 0 | 0 | 0.0 | 0.5 | 33 | 1.2 |

amount of tin depresses the dehydrogenation activity as shown in Fig. 2 for cyclohexylamine and in Fig. 3 for cyclohexane. For the dehydrogenation of cyclohexanone (Fig. 1) and 2-propanol (Fig. 4), similar results are expected in analogy with the previous work (*2*). The dehydrogenation of 2-propanol was confined to the HC–OH bond; on the contrary, the dehydrogenations of cyclohexanone, cyclohexylamine, and cyclohexane propagated to the entire structure of the six-membered ring. The influence of the catalyst composition on the dehydrogenation activity, however, was similar in the four reactions in the two catalyst systems. Therefore, whether the dehydrogenation is localized to a bond or propagated to the entire ring seems to be independent of the catalyst composition. The initial steps of the dehydrogenation of these cyclic reactants may be localized to a bond. This inference may be in accord with the results of Blakely and Somorjai (*11*). They observed the formation of cyclohexene in the dehydrogenation of cyclohexane to benzene under relatively mild conditions (423 K) at $10^{-7}$ Torr (ca. $1.33 \times 10^{-5}$ Pa) on the stepped platinum surface in flow condition. Therefore, mono-olefinic products seem to be formed in the early steps of the dehydrogenation of cyclic reactants studied here, but they were not observed, presumably, due to a high reaction temperature.

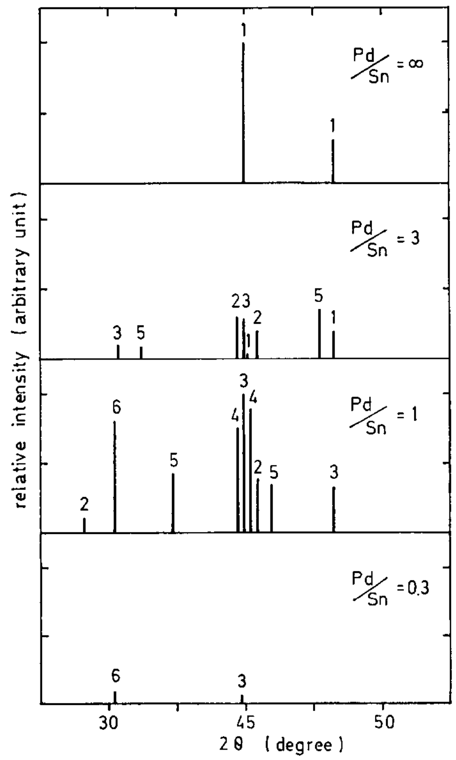

FIG. 5. X-ray diffraction patterns of reduced Pd–Sn–silica: (1) Pd, (2) $Pd_3Sn_2$, (3) PdSn, (4) $PdSn_2$, (5) $PdSn_3$, (6) β-Sn, Ni-filtered Cu*K*α.

A comparison of the activity of the catalyst of the optimum activity for the dehydrogenation reactions shows that the dehydrogenation activity decreased most quickly with cyclohexanone (Fig. 1), next with cyclohexylamine (Fig. 2), and most slowly with cyclohexane (Fig. 3). A similar tendency was observed for nickel–tin–silica (*2*). As is well known, accumulation of the carbonaceous deposit on the catalyst surface will certainly bring about a decrease in activity in connection with reaction time, especially, at a high reaction temperature and on the metallic catalysts (*12*). Rapidly decreasing activity indicates rapid deposition of carbonaceous materials. Carbonaceous materials, which are the wholly dehydrogenated–polymerized materials formed from the reaction mixture, appear to be formed rapidly from strongly adsorbed reactants. The catalysts which adsorb reactants strongly may lose their activity rapidly due mainly to the deposition of carbonaceous materials. To confirm this, the deposition of carbonaceous materials was studied kinetically. Table 3 shows the activation energy of the deposition of the carbonaceous materials in the initial 30 min. The activation energy is lower on the nickel–silica than on the nickel–tin–silica. Hence, carbonaceous materials accumulate more rapidly on tin-free or tin-poor catalysts than on tin-rich catalysts. In summary of the above, the tin-free or the tin-poor catalyst the activity of which is inherently high shows very limited activity due to the deposition of carbonaceous materials. This indicates that the amount of strongly adsorbed materials may decrease on the tin-poor catalysts. Tin will make the adsorptive ability of the catalysts weak.

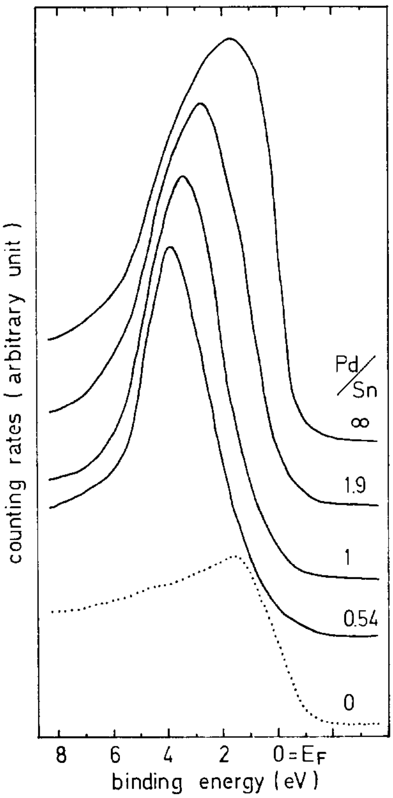

Fig. 6. XPS spectra of valence band of Pd–Sn. Maximum and minimum counts: (∞) 7431 and 1541; (1.9) 4693 and 941; (1) 3152 and 743; (0.54) 1996 and 795.

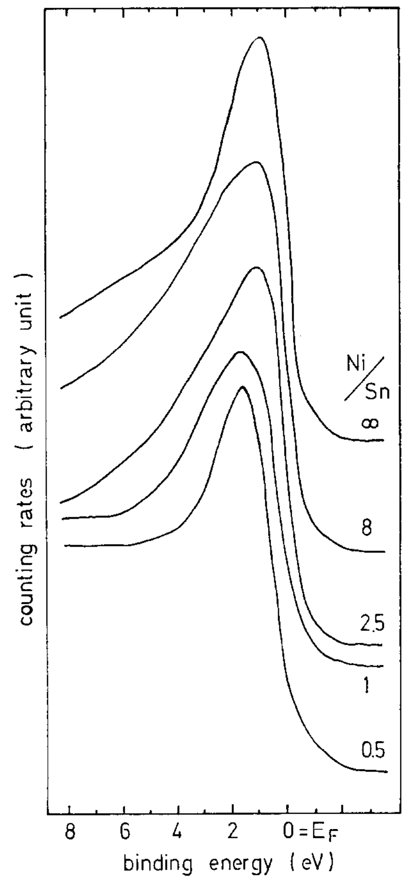

Fig. 7. XPS spectra of valence band of Ni–Sn. Maximum and minimum counts: (∞) 5298 and 868; (8) 1739 and 574; (2.5) 2340 and 669; (1) 1652 and 622; (0.5) 1105 and 774.

The hydrogenation reaction proceeds at a lower temperature than does the dehydrogenation reaction, and, therefore, a slow deposition of carbonaceous materials is expected.

Table 4 shows that both of the hydrogenations proceed almost completely on the tin-free catalysts and moderately on the tin-containing catalysts under the same reaction conditions. The rapid decrease of hydrogenation activity in connection with the decrease in the Pd/Sn and Ni/Sn ratios is noteworthy in comparison with the change in the dehydrogenation activity described above. Slow deposition of carbonaceous materials because of low temperature seems to contribute to the high activity of the palladium–silica and nickel–silica in the two hydrogenation reactions. The rapidly decreasing hydrogenation activity in connection with increasing tin concentration seems to be brought about by the weakened adsorptive ability of the tin-containing catalysts discussed above. Concerning the palladium–tin system, Clarke and Taylor have deduced that the adsorption bond between palladium and alkene is weakened by alloying with tin (*13*). With regard to platinum–tin alloy which resembles the present systems very much, Verbeek and Sachtler, using an adsorption/desorption technique, i.e., TPD, reported that no self-hydrogenation or hydrogenolysis of ethylene was observed on $Pt_3Sn$, PtSn, and $PtSn_2$ in contrast with the results obtained on Pt, on which hydrogen, methane, and ethane were produced (*14*); they also reported that a high-temperature desorption peak of ethylene observed on $Pt_3Sn$ decreased considerably on PtSn. They interpreted these results on the basis of the decrease of integral heat of adsorption of ethylene due to alloying with tin. It may be reasonable to conclude that the adsorptive ability of palladium and nickel decreases upon alloying with tin.

The observed optimum Pd/Sn and Ni/Sn ratios for the dehydrogenation reactions decrease in this order: cyclohexane (Pd/Sn = 3, Ni/Sn = 10), cyclohexylamine (Pd/Sn = 3, Ni/Sn = 8), 2-propanol (Pd/Sn = 0.3, Ni/Sn = 8), and cyclohexanone (Pd/Sn = 0.3, Ni/Sn = 2.5). The above order of the optimum composition agrees with the increasing order of the polarity of the bond through which the reactant is inferred to be adsorbed by the catalyst initially according to the discussion in the preceding part. The values of the polarity of the bond, bond moment, are as follows: C–C, 0; C–N, 0.22 *D*; C–O, 0.74 *D*; and C=O, 2.3 *D*; and carbon is on the positive side (*15*). The reactant containing the bond of the high bond moment favors the catalyst with a low adsorptive ability. The reactant which contains the bond with the high bond moment appears to be strongly adsorbed by the catalyst so that the carbonaceous materials deposit rapidly, and so that the catalyst with the low adsorptive ability is able to dehydrogenate the reactants which are liable to form the carbonaceous materials.

The surface concentration of palladium and that of nickel may be estimated from the amount of carbon monoxide adsorbed at 195 K (Table 5). The amount of carbon monoxide adsorbed by these catalysts decreased from 1 to 0.39 for a palladium concentration in the range of 100 to 23 atom% and from 1 to 0.35 in the range of a nickel concentration of 100 to 33 atom%. The amount adsorbed decreased greatly between Pd/Sn = 3 and Pd/Sn = 1 and between Ni/Sn = ∞ and Ni/Sn = 8 as shown in Table 5. The difference in the amount adsorbed is small among the tin-containing catalysts except for Pd/Sn = 3 as shown in Table 5. Although, bridge and linear types are known for the adsorbed state of carbon monoxide on palladium–silver (*16*) and also on nickel–copper (*17*), these observed values are considered a measure of the relative values of surface concentration. Noteworthy features are as follows: The amount of carbon monoxide adsorbed decreased with decrease in concentration of palladium and also of nickel; and the number of surface palladium and nickel atoms of tin-free catalysts is much greater than that expected from the amount adsorbed because the bridge type is abundant on the catalysts of palladium and nickel (*16, 17*). The adsorbed amount of carbon monoxide indicates that the difference between the surface compositions of palladium and nickel among tin-containing catalysts is small, but the difference in activity among tin-containing catalysts was observed to be not small. Therefore, we have judged the surface concentration to be a minor determining factor for catalytic activity than the above-proposed adsorptive ability of the catalysts.

Figure 6 shows that the position of the main peak associated with palladium-4d state shifts to higher binding energies as the Pd/Sn ratio decreases. The similar but smaller shift can be observed for the main peak associated with the nickel-3d state as shown in Fig. 7. The similar shift was observed with palladium–tin–silica and nickel–tin–silica, and the details will be published (*18*). The observed shift of the valence band resembles very much the shift observed on the valence bands of the following systems; i.e., nickel–germanium, iron–germanium, and gold–germanium (*4*). In these germanium alloy systems, the position and the shape of the main peak associated with the valence d-bands of nickel, iron, and gold changed gradually as the germanium content increased (*4*). It has been suggested that the shift of the main peak is brought about by the formation of bonding orbitals (*4*). This suggestion is probably appropriate for the present cases of palladium–tin and also of nickel–tin. The same tendency is also known about the valence band of the gold–tin system (*19*).

A remarkable difference can be seen between the valence band spectra of the two present systems and those of the nickel–copper system which was reported by Hüfner *et al.* (*20*). In the latter system, the valence band spectra are the superposed spectra of the valence bands of nickel and copper, and the shape of the d-band spectra does not change significantly for all compositions (*20*). This may indicate that copper atoms have little influence electronically on their nickel neighbors as Clarke reported (*21*), or that the sharing of electrons between nickel and copper is limited as discussed previously (*4*).

According to Byrne *et al.* (*22*), the value of activation energy of the hydrogen–deuterium exchange reaction on nickel–copper catalysts was kept nearly constant irrespective of the concentration of nickel, but the value of the pre-exponential factor roughly tended to decrease with decreasing nickel concentration. On this point, Takasu and Yamashina showed that the rate constant of the hydrogen–deuterium exchange on nickel–copper decreased with decrease in the surface concentration of nickel which was measured by Auger spectroscopy (*23*). Thus, the activity is altered directly by the concentration of nickel. This may be attributed to the retained d-holes at nickel atoms. The nickel d-band of nickel–copper does not appear to alter significantly in energy or shape with nickel concentration as observed by Hüfner *et al.* (*20*). The nickel d-band observed by them traverses the Fermi level at all compositions, so that there are always d-holes at nickel atoms as discussed by Clarke (*21*). Therefore, copper is merely a diluent in hydrogen–deuterium exchange on nickel–copper as Clarke discussed (*21*). It may be proposed that the density of occupied state, based on the nickel part, at the Fermi level is kept nearly constant in the nickel–copper system. Unlike these cases, the valence bands of the two present alloy systems are not the superposition of the components, but shifted to high binding energies. This shift of the valence band with increasing tin concentration may indicate a decrease in the density of the occupied state at the Fermi level. These results correspond to the weakening of the adsorptive ability with increasing tin concentration. Verbeek and Sachtler interpreted the weaker adsorption of deuterium on Pt–Sn alloys than on platinum on the basis of strong ligand effect (*14*). The ligand effect seems to explain the present results, and we propose the formation of bonding orbitals between palladium and tin and between nickel and tin as discussed above.

Bouwman *et al.* have reported the surface enrichment of platinum by the reduction of platinum–tin alloys at 773 K (*24*). With the assumption of the resemblance of platinum–tin to the two present systems, the surface composition of the present systems, i.e., of the catalysts and the XPS samples, appears to be nickel-rich or palladium-rich, because they were reduced by hydrogen just before the reaction experiment and also before the XPS observation.

According to Sinfelt *et al.* (*25*), the rate-determining step of the dehydrogenation of cyclohexane is the desorption of benzene. It may be shown by this mechanism that the weakened adsorption on the tin-containing catalysts leads to easy desorption of the dehydrogenation products, but, too great an amount of tin leads to an over-weak adsorption of the reactant. This reason, together with the decrease in carbonaceous deposits, probably accounts for the presence of the optimum composition observed in our work.

To sum up, tin brings about a similar effect on the palladium–tin and also on nickel–tin in catalytic activity and also in XPS of the valence bands discussed here. It is concluded that the role of tin in the two present catalyst systems is to make the adsorption bond weak.

## ACKNOWLEDGMENTS

The authors wish to express their thanks to Professor Kozo Hirota, Professor Emeritus of Osaka University, for helpful discussions and encouragement and to Professor Shigeru Maeno, Kobe University. The authors express their thanks to Mr. Etsuhiro Muneyama and Mr. Kenji Nomura for their cooperation in the experiments. The authors also express their thanks to Kawaken Fine Chemicals Co., Ltd. (Tokyo), for supplying metallic palladium and palladium nitrate.

## REFERENCES

*1.* Swift, H. E., and Bozik, J. E., *J. Catal.* **12**, 5 (1968).
*2.* Masai, M., Mori, K., Muramoto, H., Fujiwara, T., and Ohnaka, S., *J. Catal.* **38**, 128 (1975).
*3.* Elliot, R. P., "Constitution of Binary Alloys, First Supplement," p. 732. McGraw–Hill, New York, 1965.
*4.* Tamura, K., Fukushima, J., Endo, H., Kishi, K., Ikeda, S., and Minomura, S., *J. Phys. Soc. Japan* **36**, 565 (1974).
*5.* ASTM Powder Diffraction Cards, 5-0681.
*6.* ASTM Powder Diffraction Cards, 4-0801.
*7.* ASTM Powder Diffraction Cards, 4–0803.
*8.* ASTM Powder Diffraction Cards, 15-575.
*9.* ASTM Powder Diffraction Cards, 7-179.
*10.* ASTM Powder Diffraction Cards, 4-0673.
*11.* Blakely, D. W., and Somorjai, G. A., *J. Catal.* **42**, 181 (1976).
*12.* Bond G. C., "Catalysis by Metals," p. 407. Academic Press, London and New York, 1962.
*13.* Clarke, J. K. A., and Taylor, J. F., *J. Chem. Soc. Faraday Trans. I* **72**, 917 (1976).
*14.* Verbeek, H., and Sachtler, W. M. H., *J. Catal.* **42**, 257 (1976).
*15.* Smyth, C. P., "Dielectric Behavior and Structure," p. 244. McGraw–Hill, New York, 1955.
*16.* Soma-Noto, Y., and Sachtler, W. M. H., *J. Catal.*, **32**, 315 (1974).
*17.* Soma-Noto, Y., and Sachtler, W. M. H., *J. Catal.* **34**, 162 (1974).
*18.* Masai, M., Honda, K., Ohnaka, S., Kishi, K., and Ikeda, S., "$H_2$–$D_2$ Exchange Reaction on Ni–Sn–$SiO_2$ and Pd–Sn–$SiO_2$ Catalysts, An XPS Approach." Proceedings, 7th International Vacuum Congress and 3rd International Conference on Solid Surfaces, p. 835, Vienna, Austria, September 1977.
*19.* Watson, R. E., and Perlman, M. L., *in* "Structure and Bonding" (J.D. Dunitz, P. Hemmerich, R. H. Holm, J. A. Ibers, C. K. Jørgensen, J. B. Neilands, D. Reinen, and R. J. P. Williams, Eds.), Vol. 24, pp. 83–132. Springer–Verlag, Berlin, 1975.
*20.* Hüfner, S., Wertheim, G. K., Cohen, R. L., and Wernick, J. H., *Phys. Rev. Lett.* **28**, 488 (1972).
*21.* Clarke, J. K. A., *Chem. Rev.* **75**, 291 (1975).
*22.* Byrne, J. J., Carr, P. F., and Clarke, J. K. A., *J. Catal.* **20**, 412 (1971).
*23.* Takasu, Y., and Yamashina, T., *J. Catal.* **28**, 174 (1973).
*24.* Bouwman, R., Toneman, L. H., and Holscher, A. A., *Surface Sci.* **35**, 8 (1973).
*25.* Sinfelt, J. H., Carter, J. L., and Yates, D. J. C., *J. Catal.* **24**, 283 (1972).